# *Contribution of ALOS PALSAR data for land use estimation*

**C. Lardeux[(1)], P.-L. Frison[(1)], C. Tison[(2)], J.-C. Souyris[(2)], S. Niculescu[(3)], B. Stoll[(4)], J.-P. Rudant[(1)]**

[(1)] UMLV, Institut Francilien des Geosciences 5 bd Descartes, 77454 Marne la Vallee Cedex 2, France, E-mail: lardeux@univ-mlv.fr

[(2)] CNES, 18 avenue edouard belin, 31401 Toulouse cedex 4, France.

[(3)] Université de Bretagne Occidentale, IUEM – Géomer, Technopôle Brest-Iroise Place Nicolas Copernic 29280 Plouzané Cedex, France

[(4)] UPF, Universitée de Polynésie française bp 6570, 98702 FAA'A aéroport de tahiti Polynésie française, France

***Abstract***

While they preserve some of polarimetric information as those that would be recorded by a full polarimetric (FP) radar sensor, compact polarimetry (CP) is relevant for system constraints reduction. This study focuses on the comparison between the FP mode, the CP mode as π/4 mode and the dual polarimetric mode (DP) of ALOS PALSAR.

The SVM (Support Vector Machine) algorithm has been implemented as it allows to take into account numerous and heterogeneous polarimetric indices, such as the intensity channels, the degree of coherence between different polarisation, the H/a/α parameters or the Freeman parameters obtained from the corresponding target decomposition methods.

The results obtained with AIRSAR full polarimetric data over a Polynesian island to provide a global cartography are discussed and compared to the results obtained with the simulation of the π/4 modes and the DP mode. It is shown that the contribution of the different polarimetric indicators improve significantly the classification accuracy with respect to the π/4 mode and the DP mode of PALSAR.

***Keywords:*** SAR polarimetry, compact polarimetry, classification.

## 1. INTRODUCTION

The overall goal of this study is to assess the potential of polarimetric SAR data for land-use estimation over tropical vegetation. The study site is the Tubuai Island in French Polynesia for which local authorities are concerned with vegetation inventory. Full polarimetric data have shown their potential for the cartography of the vegetation from AIRSAR acquisitions that have been realised in 2000 over this area. The acquisition of ALOS data will allow to update the vegetation cartography, in particular for the monitoring of invasive species. In order to optimize the future ALOS acquisition modes, the focus is put on the evaluation of dual polarisation mode with respect to the full polarisation mode and compared to the π/4 mode [1].

When dealing with classification methods applied to full polarimetric data, the Wishart classification [2] is generally used. In order to combine numerous and heterogeneous polarimetric indices derived from single or multy-frequency polarimetric SAR data, the SVM (Support Vector Machine) classification method [3] is implemented. This later is especially well suited to handle linearly non separable case by using Kernel functions.

The study area and the dataset are presented in the second part of this paper. The third part details the SVM algorithm [3] and describes the different polarimetric indices used in the classifications. The results are presented in the last part of the paper.

## 2. STUDY AREA AND DATASET

### 2.1 The Tubuai Island

French Polynesia islands are located at the middle of the South Pacific Ocean. They are quickly evolving in the tourism industry, and from the economic and geostrategic points of view. They are subject to a strong environmental planning leading to landscape changes as well to the introduction of invasive species. Consequently, the local administration is involved in the global cartography and inventory of the Polynesian landscape leading to support an AIRSAR mission. We focus on data acquired over the Tubuai Island, in the Australes Archipelago at the South of French Polynesia. Tubuai is a 45 $km^2$ island with a population of about 6000 inhabitants. It is particularly relevant because of its great landscape diversity: several types of forests, agricultural fields, and some residential areas scattered along the coast. Different land use classes are present, including 4 forest classes: *Hibiscus tiliaceus* (also called Purau), *Pinus Caribeae* (also called Pinus), *Paraserianthes Falcataria* (also called Falcata) and *Psidium Cattleianum* (called Guava). The latter is particularly watched as it is an invasive species. The "low vegetation" is composed by 2 classes: the fern land and the swampy vegetation. The last class describe the bare soils. Several ground surveys has been carried out, and a Quickbird image acquired in August 2004 is also available to supply an accurate validation data set over the entire island. The classes are summarized in Tab 1. The ground surveys allow the definition of different regions of interest. They are randomly divided in 2 distinct subsets, one defining the training and the other the control dataset. The

training and control pixels number is the same for each class and is also given in Tab 1.

*Table 1. Vegetation classes of the Tubuai Island*

| Vegetation type | Vegetation Class | Training/control pixels number |
|---|---|---|
| Forest | *Pinus* | 5322 |
| | *Falcata* | 2589 |
| | *Purau* | 6186 |
| | *Guava* | 348 |
| low vegetation | Fern land | 2191 |
| | Swamp | 5511 |
| | No vegetation | 4445 |

### 2.1.2 Dataset

An AIRSAR airborne mission took place in August 2000 over the main Polynesian islands. The AIRSAR data were acquired over the Tubuai Island along 2 passes in reverse path, in Polsar mode. The data set used in this study consists in full polarimetric data in L ($\lambda$ = 23 cm) and P ($\lambda$ = 67cm) bands with an additional C band channel ($\lambda$=5.7cm) in VV polarization. Full polarimetric data are delivered in MLC (Multi Look Complex) format, corresponding to about 9 looks, with a resolution of 5 meters. The relative phase of the original data has been calibrated [4] and an intensity bias has been corrected both in L and P bands values to retrieve expected $\sigma^0$ value over dense forest areas.

## 3. METHODOLOGY

### 3.1 SVM

The SVM is a classification algorithm based on the searching the best surface separating the training samples. Each input data are defined by a vector composed by the so called primitives, which, in our case, are the polarimetric indices. The interest of the SVM is the use of the kernel function that handles separable heterogeneous and noisy data as shown in the Fig 1. More details about the SVM algorithm can be found in [3] and [5].

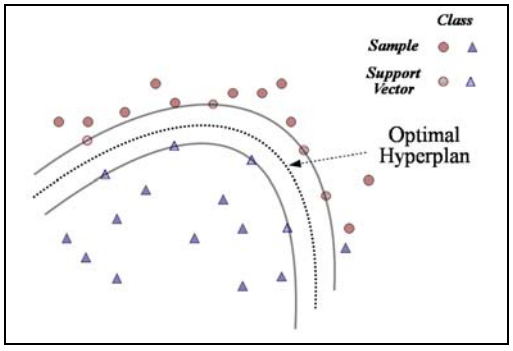


*Figure 1. SVM : Non linear case*

### 3.2 Polarimetric indices

Full polarimetric sensor allows determining the covariance matrix C. This latter is constructed from the scattering vector $k_l$ expressed in the lexicographic basis as follows:

$$k_l = \begin{pmatrix} S_{pp} \\ \sqrt{2}S_{pq} \\ S_{qq} \end{pmatrix}, \quad C = \left\langle k_l . k_l^T \right\rangle \quad (1)$$

where $S_{pq}$ denotes the scattering matrix element corresponding to the *p-q* polarization of the receiving-transmitting wave (*p,q* referring to horizontal, h, or vertical, v, linear polarization), <.> stands for he spatial averaging made during the multi-look process. Many different polarimetric indices are extracted from the covariance matrix. In a previous study ([5], the contribution of the polarimetric indices as been assessed through an iterative algorithm based on the so-called greedy backward methods [6]. The greedy backward algorithm removes step by step the less efficient components (based on the mean of the producer accuracy (MPA) of the classification) of an initial vector configuration.

The results showed that a subset of polarimetric indices is particularly discriminating, which allow to define the V1 Vector to be use in the SVM algorithm. These are presented below and summarized in the Tab 2.

- The modulus and the phase of the polarimetric degrees of coherence [7]

  $\rho_{hh-vv}$ , $\rho_{hv-vv}$ , $\rho_{hv-hh}$ , $\rho_{ll-lr}$ , $\rho_{rr-lr}$ , $\rho_{ll-rr}$ ,
  computed over a 3x3 neighbourhood as follow:

  $$\rho_{pq-p'q'} = \frac{\left\langle S_{pq} . S_{p'q'} \right\rangle}{\sqrt{\left\langle \left| S_{pq} \right|^2 \right\rangle . \left\langle \left| S_{p'q'} \right|^2 \right\rangle}} \quad (2)$$

  where p, q, p', q' stands for h, v, l or r polarization.

- The 3 parameters $H/A/\alpha$ representing the entropy, the scattering mechanism, and the anisotropy estimated from the Cloude and Pottier decomposition [8].
- The 3 intensity parameters $P_s$, $P_d$, $P_v$, corresponding to the weight of single, double and volume contribution in the backscattered response of the Freeman decomposition [9].
- The texture is taken into account through the coefficient of variation $c_v = \frac{\sigma}{\mu}$, $\sigma$ and $\mu$ are representing the standard deviation and mean of the intensities in the linear and circular polarization computed over a 5x5 neighbourhood.

At the exception of the coefficient of variation $c_v$, all the other polarimetric indices have been estimated after the application of a polarimetric filter [10] to original data.

*Table 2. Vector configuration of the FP and π/4 mode*

| V1 | V2 | V3 |
|---|---|---|
| $c_{v\text{-}vv}$, $c_{v\text{-}hv}$, $c_{v\text{-}vv}$, $c_{v\text{-}ll}$, $c_{v\text{-}lr}$, $c_{v\text{-}rr}$ | $c_{v\text{-}vv}$, $c_{v\text{-}hv}$, $c_{v\text{-}vv}$ $c_{v\text{-}ll}$, $c_{v\text{-}lr}$ | C2 |
| $\lvert\rho_{hh\text{-}vv}\rvert$, $\varphi_{hh\text{-}vv}$, $\lvert\rho_{hh\text{-}hv}\rvert$ $\varphi_{hh\text{-}hv}$, $\lvert\rho_{vv\text{-}hv}\rvert$ | $\lvert\rho_{hh\text{-}vv}\rvert$, $\varphi_{hh\text{-}vv}$ | SPAN = $\lvert S_{sp}\rvert^2 + \lvert S_{sp}\rvert^2$ |
| $\lvert\rho_{ll\text{-}rr}\rvert$, $\lvert\rho_{ll\text{-}lr}\rvert$, $\varphi_{ll\text{-}lr}$, $\lvert\rho_{rr\text{-}lr}\rvert$, $\varphi_{rr\text{-}lr}$, | $\lvert\rho_{ll\text{-}lr}\rvert$, $\varphi_{ll\text{-}lr}$ | $c_{v\text{-}pq}$, $c_{v\text{-}pq}$ $\frac{I_{pq}}{I_{pq}}$ |
| a/α | a/α | $\lvert\rho_{pq\text{-}pqv}\rvert$, $\varphi_{pq\text{-}pq}$ |
| $P_s$, $P_d$, $P_v$ | $P_s$, $P_d$, $P_v$ | H/a/α (relative to the DP mode) |
| 21 $el^{ts}$ | 14 $el^{ts}$ | 13 $el^{ts}$ |

### 3.3 Compact Polarimetry: the "π/4" Mode

The "π/4" mode consists in a transmitter polarization either circular or oriented at 45°, and in receivers that are in horizontal and vertical polarizations with respect to the line of sight [1].

Due to some symmetry properties (reflection, rotation, azimuthal) for natural media, some hypothesis can be made to reconstruct the full polarimetric information. One important hypothesis made to reconstruct the full polarimetric information is:

$$\left\langle S_{hh}.S_{hv}^{*}\right\rangle = \left\langle S_{hv}.S_{vv}^{*}\right\rangle = 0 \quad (3)$$

This property is generally observed over vegetated areas.

Consequently, some polarimetric parameters loose their signification, or become redundant with other. For example, the circular intensities $I_{ll}$ and $I_{rr}$ are equal. In the same way, the degree of coherence $\rho_{ll\text{-}rr}$ has no more interest, as well as the degree of coherence involving the cross linear polarisation hv that is equal to zero. The corresponding polarimetric indices obtained from the V1 vector with such restriction define the V2 vector that is summarized Tab 2.

### 3.3 Dual polarimetric mode (PALSAR)

The dual polarimetric mode of ALOS PALSAR consists in the emission of the wave in one linear polarization with a reception in two linear polarizations. Consequently, the result is a couple of intensities of 2 linear configurations (*i.e.* hh/hv, vv/hv or hh/vv) with the addition of the phase difference between the 2 polarisations. Then the corresponding covariance matrix C2 is composed by 3 non zero elements, 2 of whom are diagonal (*i.e.* 4 non zero coefficients). The different polarimetric indices that can be derived from such measurements define a vector V3 which is detailed in Tab 3. It can be noticed that the H/a/α parameters estimated for the DP mode are relative to the diagonalization of the 2x2 matrix C2 and are consequently less relevant than those computed with the FP mode relative to the 3x3 matrix.

## 4. RESULTS AND DISCUSSION

The overall performance of the classification is given by the Mean of the Producer Accuracy (MPA), while the Producer Accuracy is used to estimate the performance for the different classes.

The results obtained at L band in the FP mode are compared to those obtained with simulation of the π/4 and DP modes of PALSAR. In addition, to investigate the expected added value of an additional ASAR acquisition for example, for each mode the intensity and the texture coefficient of the VV polarisation of the C band are added. Results are summarized in Tab 3. Also are shown for indication the results obtained with Alternate Polarisation (AP) mode like defined on the ASAR sensor (*i.e.* 2 linearly polarised intensities only, with no differential phase).

*Table 3. SVM classification results for the FP, DP and AP modes for L band and L+$C_{VV}$: MPA (%)*

| | | **L band** | **L band+$C_{VV}$** |
|---|---|---|---|
| **FP** | | 92 | 97 |
| **π/4** | | 79 | 92 |
| **PALSAR DP** | HH/HV | 77 | 89 |
| | VV/HV | 69 | 86 |
| | HH/VV | 78 | 92 |
| **ASAR AP** | HH/HV | *59* | *81* |
| | VV/HV | *53* | *75* |
| | HH/VV | *59* | *80* |

When only the L band is concerned, the classification accuracy of the FP mode with the SVM algorithm (92%) is improved of more than 20% with respect to the Wishart algorithm (MPA= 69%). It shows the interest of the SVM algorithm for the classification of FP data.

Among the different partial polarimetric modes, the π/4 mode gives the best accuracy with a MPA value of 79%, (*i.e.* 13% lower than the FP mode). Similar results are obtained with the HH/HV (77%) and HH/VV (78%) DP mode. The lost of the differential phase between the 2 linear polarisation channels, as in the AP mode, lead to a strongly reduced classification accuracy with MPA value of 59%, that is 33% lower than with FP mode. It can be noticed that the VV/HV configuration for both DP and AP modes show the lowest results.

The VV/HV is the less performant among the DP modes with a MPA 20% lower than the FP mode.

The Producer Accuracies of the different vegetation classes are detailed in Tab 4 for the L band. It is shown that only the FP mode is able to discriminate between the different forest classes. The partial polarimetric data introduce significant confusion between the forest classes with a PA lower than 79% for the 4 forest classes. Among the different forest classes, the "Guava" and "Falcata" are especially difficult to be discriminated. On the contrary, the partial polarimetric modes allow a good discrimination between the 3 vegetation types that are "bare soils", "low

vegetation", and 'forest" as testify the MPA of 94% obtained when only these 3 land use types are investigated.

The addition of the C band VV intensity and coefficient of variation improves significantly the performance of the DP and π/4 modes with a MPA of 92% that is only 5% lower than for similar configuration involving full polarimetric data at L band (97%). This increasing is due to the better discrimination between the forest classes, as it is detailed in Tab 5. The MPA value obtained over only the 4 forest classes is now of 86% with respect to 63% when only the L band DP mode is used. The combination of the C band to AP mode at L band gives performance about 10% lower than the previous configuration (see Tab. 3). The lower performance of the AP mode principally comes from the unability to discriminate the "Fern land" from the "swampy vegetation" (not shown here).

Finally the FP mode gives very good results in all the classes with some confusion for the Falcata.

*Table 4. SVM classification results for the FP, DP for L band: MPA (%)*

| | | FP | π/4 | HH/HV | VV/HV | HH/VV |
|---|---|---|---|---|---|---|
| ***Forest*** | Pinus | 87 | 66 | 65 | 66 | 67 |
| | Falcata | 82 | 61 | 55 | 23 | 54 |
| | Purau | 89 | 77 | 77 | 77 | 79 |
| | Guava | 91 | 66 | 59 | 58 | 65 |
| ***Low vegetation*** | Fern land | 98 | 87 | 87 | 70 | 88 |
| | Swamp | 100 | 97 | 97 | 95 | 98 |
| ***No vegetation*** | | 99 | 96 | 95 | 94 | 97 |
| **MPA** | | **92** | **79** | **77** | **69** | **78** |

*Table 5. SVM classification results for the FP, DP for L band+$C_{VV}$: MPA (%)*

| | | FP | π/4 | HH/HV | VV/HV | HH/VV |
|---|---|---|---|---|---|---|
| ***Forest*** | Pinus | 99 | 98 | 98 | 98 | 98 |
| | Falcata | 90 | 81 | 77 | 60 | 78 |
| | Purau | 97 | 92 | 92 | 91 | 93 |
| | Guava | 94 | 86 | 72 | 74 | 82 |
| ***Low vegetation*** | Fern land | 98 | 91 | 92 | 84 | 94 |
| | Swamp | 100 | 98 | 98 | 97 | 99 |
| ***No vegetation*** | | 99 | 97 | 97 | 96 | 98 |
| **MPA** | | **97** | **92** | **89** | **86** | **92** |

## 5. CONCLUSIONS

This study shows the interest of the full polarimetry data for the cartography in tropical environments. The simulation of different compact polarimetric modes like π/4 and ALOS DP (in HH/HV and HH/VV configuration) show similar results. When only L band is considered, it allows the discrimination of "forest", "low vegetation", and "no vegetation" classes. However, when C band in VV polarisation is added to the L band (corresponding for example to one PALSAR plus one ASAR acquisitions) the results are significantly improved for the forest classes, leading to MPA lower of only 5% with respect to FP mode. The lost of the differential phase between the two linear polarization channels acquisition, as in the case of ASAR AP mode reduces significantly the classification performance. In both DP and AP modes, the VV/HV acquisition shows the poorest performance with respect to HH/HV and HH/VV configurations.

**Acknowledgement**

The authors are grateful to Jean-Yves Meyer for the survey mission and thank the Government of French Polynesia and its Urbanism Department for providing the AirSAR, MASTER and Quickbird data required for this study.

**References**

[1] J.-C. Souyris, P. Imbo, R. Fjørtoft, S. Mingot, J.-S. Lee, "Compact Polarimetry Based on Symmetry Properties of Geophysical Media: The π/4 Mode," IEEE Trans. Geosci. Remote Sens., vol. 43, no. 3, Mar. 2005. Page(s):634 – 646

[2] J. S. Lee, M. R. Grunes, R. Kwok, "Classification of multi-look polarimetric SAR imagery based on complex Wishart distribution," Int. J. Rem. Sens., vol. 15, n° 11, 1994, 2299-2311.

[3] C. J. Burges, "A tutorial on support vector machines for pattern recognition, in Data mining and knowledge discovery," U. Fayyad, Ed. Kluwer Academic, 1998, pp. 1-43.

[4] H. A. Zebker, J. J. van Zyl, and D.H.Held, "Imaging radar polarimetry frow waves synthesis," J.Geophy. Res, vol. 91, no B5. pp. 683-701, Jan. 1987.

[5] C. Lardeux, P-L. Frison, C. Tison, D. Deleflie, J-C. Souyris, J-P. Rudant, B. Stoll, "Comparison of compact polarimetric with full polarimetric radar data for land use discrimination based on SVM classification," Proc. POLinSAR, Frascati, Italie, Jan. 2007

[6] Guyon, I., Weston, J., Barnhill, S., & Vapnik, V., "Gene selection for cancer classification using support vector machines./ Machine Learning," 46/(1-3), 389-422, 2002.

[7] Mattia F., Le Toan T., Souyris J.-C., De Cariolis G., Floury N., Posa F., Pasqueriello G., "The effect of surface roughness on multifrequency polarimetric SAR data," IEEE Trans. Geosci. Remote Sensing, vol. 35, n° 4, pp 954-966, 1997.

[8] S. R. Cloude, E. Pottier, "A Review of Target Decomposition Theorems in Radar Polarimetry," IEEE TGRS, vol. 34, no. 2, pp 498-518, Sept. 1995.

[9] A. Freeman and S. L. Durden, "A three-component scattering model for polarimetric SAR data," IEEE Trans. Geosci. Remote Sens., vol. 36, no.3, pp. 963-973, May 1998.

[10] J. S. Lee, M. R Grunes, G. de Grandi, "Polarimetric SAR speckle filtering and its implication for classification," IEEE Trans. Geosci. and Rem. Sens., vol. 37, n0 5, 1999, 2362-2373.